07

Linear Fresnel lenses with optimized photocurrent density distribution on the surface of multi-junction solar cells

© N.A. Sadchikov, A.V. Andreeva

Ioffe Institute, St. Petersburg, Russia
E-mail: N.A.Sadchikov@mail.ioffe.ru

Received July 29, 2025
Revised August 20, 2025
Accepted August 22, 2025

A combined linear Fresnel lens with optimized photocurrent density distribution in the focal spot has been developed for use in concentrator modules for space applications. In a combined Fresnel lens, the focal lengths of each microprism are selected individually based on the proposed algorithm, which made it possible to reduce the heterogeneity in the profile of the photocurrent density distribution in the central region on the surface of InGaP/InGaAs/Ge and AlInGaP/AlInGaAs/InGaAs/Ge solar cells, as well as increase the peak values of the photocurrent density in the center of the focal spot.

Keywords: linear Fresnel lens, multi-junction solar cell, solar radiation concentrators, space solar panels.

DOI: 10.61011/TPL.2025.11.62219.20458

The possibility of application of concentrator photovoltaic modules (CPVs) based on linear Fresnel lenses (FLs) operating in tandem with multi-junction solar cells (MJSCs) in solar batteries for spacecraft [1–8], including those tested in successful deep-space flights [7,8], has been discussed for many years. The use of CPVs allows one to reduce the number of needed MJSCs, which are highly efficient but expensive, by a factor proportional to the solar radiation (SR) concentration ratio [1,2,4–8]. Lens panels with linear FLs are fabricated by polymerizing a radiation-resistant silicone compound between a negative master matrix, which is manufactured by diamond micro-turning, and thin quartz glass, which serves as a base for the silicone compound with a Fresnel profile. In commercial production, one may use the well-proven technology of fabrication of polyurethane copies with a negative Fresnel profile.

The most important advantage of FL-based SR concentrators used in solar batteries of this type is the increase in efficiency and radiation resistance due to an increase in MJSC efficiency through SR concentration and a suppression of the influence of space factors (fluxes of electrons and high-energy ions, etc.) on MJSCs, which helps slow down the degradation of semiconductor structures of MJSCs. Modern MJSCs reach their peak efficiency at solar radiation concentration ratios exceeding 100x; the increase in efficiency becomes noticeable at ratios in excess of 5x [2,3,6,7]. At the same time, the restrictions on mass-dimensional parameters of CPVs intended for space use limit the concentration ratio and the focal length of FLs to 10x and a value comparable to the FL aperture, respectively [1,2,4,6–8]. Therefore, it is important to develop optical concentrators with spectral homogeneity and increased peak SR concentration and photocurrent density at the center of the focal spot.

At low levels of SR concentration on the MJSC surface, the main factors reducing the efficiency of concentrator modules are chromatic aberration, which translates into heterogeneity of the profile of SR and photocurrent density distribution for different $p-n$ junctions [4,5], and recombination losses of current carriers due to low MJSC illumination levels [2,9]. The lower the SR concentration ratio is, the more significant is the contribution of recombination losses. The use of short-focus FLs enhances further the negative impact of chromatic aberration [4].

A method for mitigating the negative effect of chromatic aberration in radial FLs through proper selection of profile parameters (a table with angles and sizes of microprisms) for FLs with given size and focal length characteristics was proposed in [5,10,11]. The refraction index, the values of which are taken from dispersion dependence $n(\lambda)$ for the optical material, is a variable parameter that is used to form the FL angle table. The optimization criterion is the maximum average radiation concentration $C_{\max\, av}$ corresponding to the minimum focal spot diameter $d_{\min}$. It was demonstrated that a set of material and FL parameters has a unique corresponding value of refraction index n_{opt} for the FL profile that ensures the maximization of $C_{\max\, av}$ and $d_{\min}$.

This method was used in [4] to shape the parameters of a short-focus linear FL with a transverse size of 25 mm and a calculated focal length of 32 mm. A minimum photocurrent was provided by the middle InGaAs-based $p-n$ junction operating within the spectral range of 640–900 nm; the calculated refraction index n_{opt} was equal to its value at $n(\lambda) = 775$ nm and 50 °C.

A classical short-focus linear FL with a profile calculated in accordance with the procedure outlined in [5,10], which made it possible to achieve a peak SR concentration of 50x at the center of the focal spot, was discussed in [4,12]. This SR concentration ratio falls within the range where the maximum MJSC efficiency still cannot be reached [3].

Owing to the influence of chromatic aberrations, the values of local SR concentration and, consequently, the photocurrent densities for different $p-n$ junctions differ by tens of percent over the entire MJSC surface [4,12].

An optimized method for suppressing the influence of chromatic aberration, where the parameters of each microprism are chosen separately to shape the profile of a linear Fresnel lens (combined FL [11,12]), is proposed below. In contrast to [12], where the focal length and transverse size of a microprism were adjusted, only the angle of inclination of a microprism (focal length) is varied in the present study, while the Fresnel profile step remains constant at 0.25 mm. The values of parameters of a linear FL used for calculations are as follows: the transverse size is 25 mm, the design focal length is 32 mm, and the photosensitive MJSC area is 5×5 mm in size. The transverse size and the focal length of a linear FL were taken from performance specifications provided by the industrial partner as part of a joint project on CPV design with linear FLs [4].

The ray tracing method used in [4,5,10–12] is applied in calculations of the distribution profile of solar radiation at the focus of the Fresnel lens. The main criterion for shaping the Fresnel profile is minimization of the difference between the values of photocurrent density of individual $p-n$ junctions at the MJSC center and the transverse size of the focal spot for each $p-n$ junction with an SR interception coefficient of 90 %.

The linear FL profile was shaped for MJSCs with three $p-n$ junctions (InGaP/GaAs/Ge) and four $p-n$ junctions (AlInGaP/AlInGaAs/InGaAs/Ge). Their spectral sensitivity values were taken from [13,14]. The photocurrent densities for each $p-n$ junction of these MJSCs irradiated with cosmic spectrum AM0, 1366.1 W/m^2, are listed in Table 1.

The program for calculating the FL parameters allows one to analyze the influence of different designs of a linear FL (both classical and combined [11,12]) on the distribution profile of SR and the photocurrent density of both the complete FL and individual microprisms. The table of angles of a classical FL and the corresponding profiles for each $p-n$ junction were taken as a basis for shaping the combined FL profile. The angles of inclination of microprisms are then varied (starting from the outermost microprism) alternately upwards and downwards relative to the angle corresponding to the microprism with the same distance from the center as in the classical FL profile. The gradient descent method was used to adjust the inclination angle. At the first stage, the transverse size of the focal spot was minimized for each microprism. At the second stage of calculations, the inclination angles were varied with a smaller amplitude in order to minimize the difference between the values of photocurrent density at the MJSC center for the entire FL.

Table 1. Photocurrent densities for $p-n$ junctions of two types of MJSCs: InGaP/GaAs/Ge and AlInGaP/AlInGaAs/InGaAs/Ge (uniform irradiation, AM0 spectrum, 1366.1 W/m^2)

MJSC, 3-junction, $p-n$ junction	Photocurrent density, mA/cm^2	MJSC, 4-junction, $p-n$ junction	Photocurrent density, mA/cm^2
InGaP	16.8	AlInGaP	14.3
GaAs	17.6	AlInGaAs	14.8
Ge	25.6	InGaAs	15.9
–	–	Ge	15.3

Figure 1 shows the photocurrent density distribution profiles on the surface of two types of InGaP/GaAs/Ge MJSCs: with classical (a) and combined (b) linear FLs. Figures 2, a, b present the corresponding photocurrent density distribution profiles formed by the outer microprism of the linear FL.

Figures 3 and 4 present the photocurrent density distribution profiles on the surface of the AlInGaP/AlInGaAs/InGaAs/Ge MJSC for the complete classical (a) and combined (b) linear FLs (Fig. 3) and the photocurrent density distributions formed by the outermost microprism of the classical (a) and combined (b) linear FLs (Fig. 4).

It should be noted that the outermost microprisms have the largest inclination angle, which translates into the maximum chromatic aberration from the outermost FL region (Fig. 2, a and 4, a) and, consequently, the maximum spectral and spatial inhomogeneity of SR in the focal spot of the complete FL. It is evident from Figs. 2, b and 4, b that the size of the corresponding focal spot for each $p-n$ junction and the difference in peak photocurrent density values of the corresponding SR subrange may, however, be reduced by choosing the optimal inclination angle for the outermost microprism. The transverse size of the focal spot formed by each microprism and the non-uniformity of photocurrent density decrease for all individual microprisms as one moves from the edge to the center of the FL. This translates into a reduction of the focal spot size and an increase in peak photocurrent density for the complete FL (Figs. 1, b and 3, b). This is the mechanism behind the redistribution of SR to the central MJSC region observed when the combined FL profile is used.

With the classical approach to shaping the profile of a short-focus linear FL, the inclination angles of each microprism are suboptimal in terms of the above criteria, since a limit in reducing the influence of chromatic aberration in the distribution profile of SR and photocurrent density on the MJSC surface was reached when the refraction index was varied as a design parameter [4,5,11,12] and a table of angles was formed for the entire FL in a single step.

The data on local SR concentration ratio are intermediate and are used to calculate the values of photocurrent density. With the combined lens, the maximum peak concentration of solar radiation at the solar cell center is 60.5x for the InGaAs/GaAs/Ge MJSC and 53x for the AlInGaP/AlInGaAs/InGaAs/Ge MJSC. Compared to the classical lens, the SR concentration ratio over the entire solar cell area increases by 15 % on average.

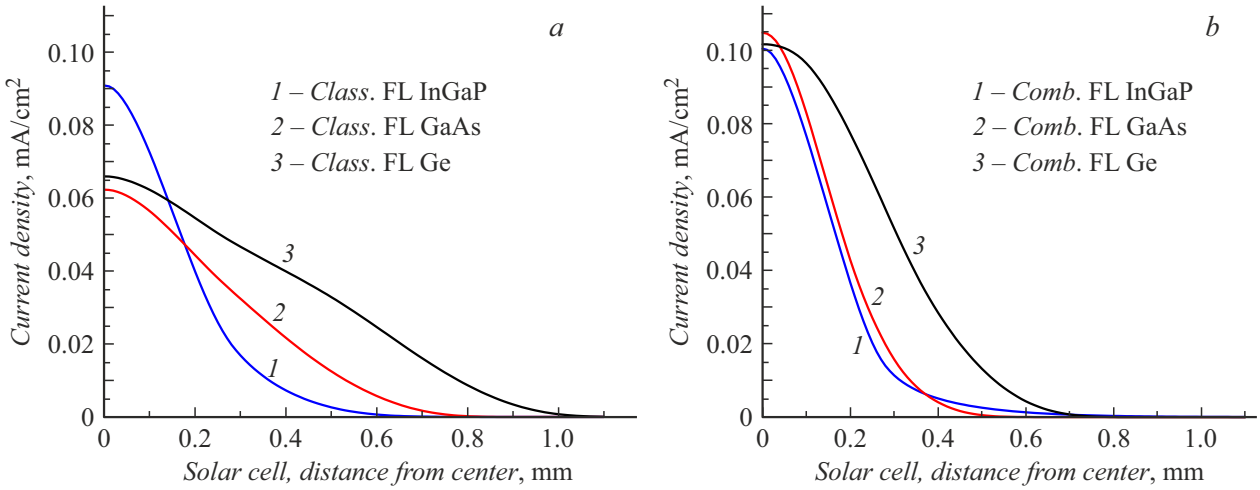

Figure 1. Photocurrent density distribution profiles on the InGaP/GaAs/Ge MJSC surface from the MJSC center to the edge. *a* — Classical FL; *b* — combined FL.

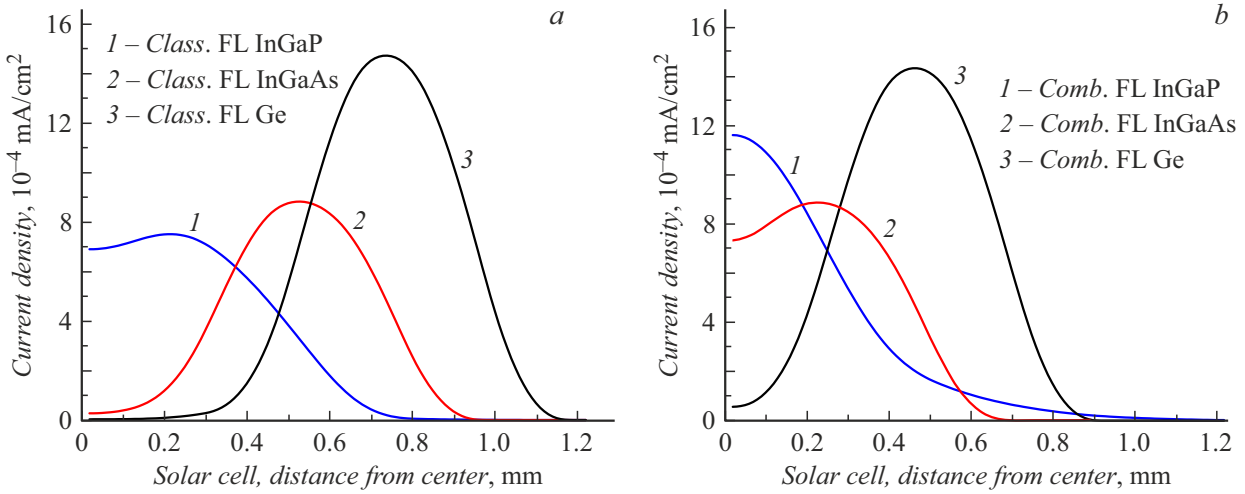

Figure 2. Photocurrent density distribution profiles on the MJSC surface formed by the outermost microprism of a linear FL located in the region most distant from the center. *a* — Classical FL; *b* — combined FL.

Table 2 lists the main parameters of the photocurrent density distribution profiles for the classical and combined FLs and two MJSC types: the peak photocurrent density at the center of the focal spot for each $p-n$ junction, the ratio between the maximum and minimum peak current density values, and the size of the focal spot with an interception coefficient of 90 %.

It should be noted that InGaAs/GaAs/Ge and AlInGaP/AlInGaAs/InGaAs/Ge MJSCs differ in the nature of the photocurrent density distribution profile for the combined linear FL. In the former case, the difference between the current density values at the center of the focal spot is minimal (Fig. 1, *b*), while a certain discrepancy between these values at the center of the spot still remains in the latter case (Fig. 3, *b*).

These differences between the two photocurrent density distribution profiles are attributable to different ratios of the current density values of individual $p-n$ junctions in the spectral sensitivity of two types of solar cells (Table 1). The InGaAs/GaAs/Ge MJSC has a large spread of current density values from 16.8 to 25.6 mA/cm^2, while the spread for the AlInGaP/AlInGaAs/InGaAs/Ge MJSC is much less significant (from 14.3 to 15.9 mA/cm^2). The same algorithm for generating the Fresnel profile was used in these two designs. The difference lies only in the number of spectral subranges that corresponds to the number of $p-n$ junctions. Trying different optimization options, we arrived at a design in which the alignment of peak photocurrent densities at the center of the focal spot for the AlInGaP/AlInGaAs/InGaAs/Ge MJSC led to an almost zero difference between these values (as in the InGaAs/GaAs/Ge MJSC). However, significant blurring of the focal spot and an almost 1.5-fold reduction of the peak values were also observed in this case. The presented photocurrent density

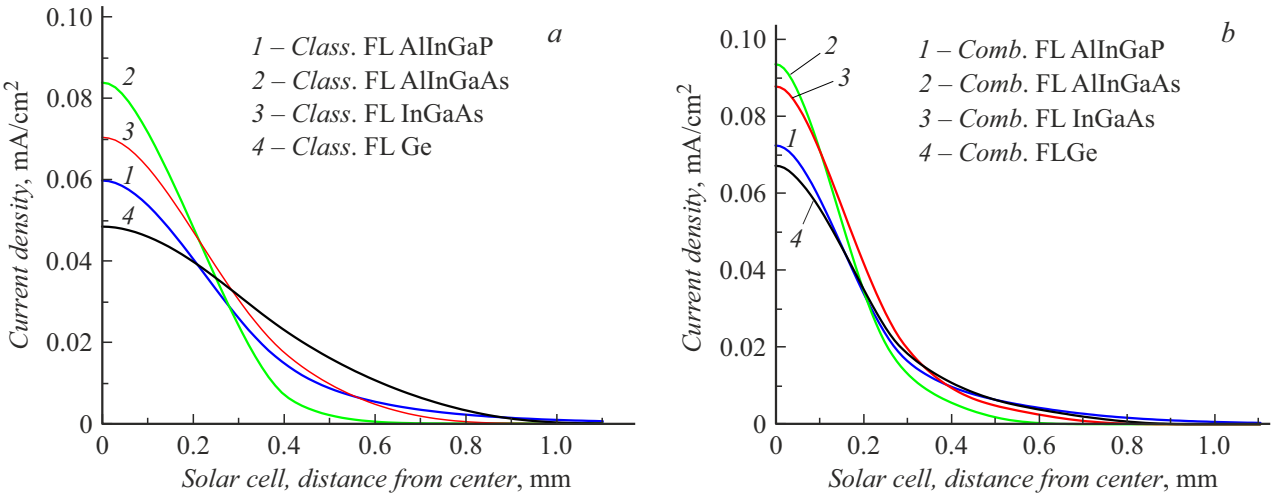

Figure 3. Photocurrent density distribution profiles on the AlInGaP/AlInGaAs/InGaAs/Ge MJSC surface. *a* — Classical linear FL; *b* — combined linear FL optimized for maximum photocurrent density at the center of the focal spot.

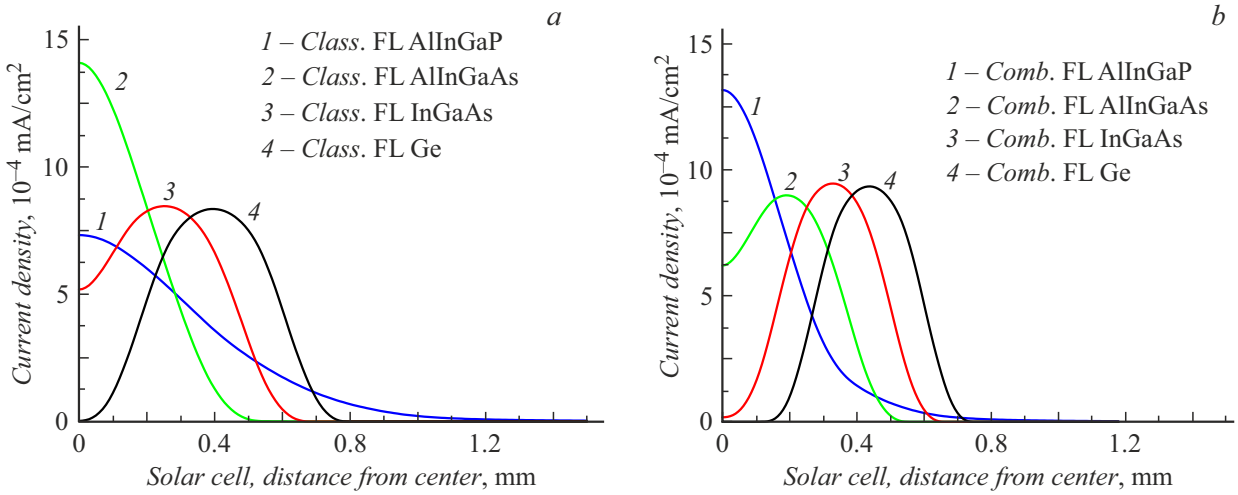

Figure 4. Photocurrent density distributions on the AlInGaP/AlInGaAs/InGaAs/Ge MJSC surface formed by the outermost microprism of a linear FL located in the region most distant from the center. *a* — Classical FL; *b* — combined FL.

distribution profiles (Figs. 1, *b* and 3, *b*) were judged to be optimal in the context of the present research, which was aimed at increasing the peak values of photocurrent density and reducing the size of the focal spot. It is evident that the spectral sensitivity of the MJSC (the difference in photocurrent density values for each $p-n$ junction) in an FL−MJSC pair imposes certain constraints on the potential results of FL optimization.

The combined short-focus linear FL allowed us to reduce significantly the difference in photocurrent density values for different $p-n$ junctions at the center of MJSCs with three and four $p-n$ junctions and to increase the peak photocurrent density values at the central part of the focal spot (compared to the classical short-focus linear FL). While the ratio of peak values of the minimum and maximum photocurrent density $I_{peak\ \max}/I_{peak\ \min}$ for the classical LF coupled with the InGaAs/GaAs/Ge MJSC is 1.46, the corresponding ratio for the combined FL is 1.05 (Fig. 1, Table 2).

In the linear FL−AlInGaP/AlInGaAs/InGaAs/Ge MJSC pair, the difference in peak photocurrent density values was also suppressed: $I_{peak\ \max}/I_{peak\ \min} = 1.39$ (the corresponding ratio for the classical FL is 1.74).

With the combined FL, the transverse size of the focal spot with an SR interception coefficient of 90 % decreased by a factor of 1.5 for the InGaAs/GaAs/Ge MJSC and by 20 % for the AlInGaP/AlInGaAs/InGaAs/Ge MJSC (Table 2).

Conflict of interest

The authors declare that they have no conflict of interest.

Table 2. Peak photocurrent density at the center of two types of MJSCs for classical and combined FLs; ratio between the maximum and minimum photocurrent densities $I_{peak\,max}/I_{peak\,min}$ ($I_{peak\,max}$ is the highest photocurrent density at the center of the focal spot and $I_{peak\,min}$ is the lowest photocurrent density at the center of the focal spot); transverse size of the focal spot with an SR interception coefficient of 90 %

MJSC, 3-junction, $p-n$ junction	InGaP	GaAs	Ge	–
Photocurrent density at the MJSC center for classical/combined FLs, mA/cm^2	0.091/0.1	0.062/0.105	0.066/0.101	–
$I_{peak\,max}/I_{peak\,min}$ for classical/combined FLs, rel. un.	1.46/1.05			
Transverse size of the focal spot for classical/combined FLs, mm	1.52/0.96			
MJSC, 4-junction, $p-n$ junction	AlInGaP	AlInGaAs	InGaAs	Ge
Photocurrent density at the MJSC center for classical/combined FLs, mA/cm^2	0.084/0.072	0.07/0.094	0.06/0.088	0.048/0.067
$I_{peak\,max}/I_{peak\,min}$ for classical/combined FLs, rel.un	1.74/1.39			
Transverse size of the focal spot for classical/combined FLs, mm	1.34/1.12			

References

[1] V.D. Rumyantsev, O.I. Chosta, V.A. Grilikhes, N.A. Sadchikov, A.A. Soluyanov, M.Z. Shvarts, V.M. Andreev, in *Proc. of 29th IEEE Photovoltaic Specialists Conf.* (IEEE, 2002), p. 1596–1599. DOI: 10.1109/pvsc.2002.1190920

[2] J. Pritchard, K. Simon, C. Dowd, E. Joshi, PAM Rev., **3**, 2 (2016). DOI: 10.5130/pamr.v3i0.1413

[3] A.A. Abushattal, A.G. Loureiro, N.E.I. Boukortt, Micromachines, **15**, 204 (2024). DOI: 10.3390/mi15020204

[4] V.S. Kalinovskii, E.A. Ionova, A.V. Andreeva, E.V. Kontrosh, V.M. Andreev, AIP Conf. Proc., **2149**, 070007 (2019). DOI: 10.1063/1.5124206

[5] M.Z. Shvarts, V.M. Emelyanov, M.V. Nakhimovich, A.A. Soluyanov, V.M. Andreev, AIP Conf. Proc., **2149**, 070011 (2019). DOI: 10.1063/1.5124210

[6] M. O'Neill, in *Fourth Int. Conf. on solar concentrators* (El Escorial, Spain, 2007). https://www.markoneill.com/ICSC4-CMLMJ-2007.pdf

[7] M.F. Piszczor, S.W. Benson, D.A. Scheiman, D.B. Snyder, H.J. Fincannon, S.R. Oleson, G.A. Landis, in *2008 33rd IEEE Photovolatic Specialists Conf.* (IEEE, 2008), p. 1–5. DOI: 10.1109/pvsc.2008.4922856

[8] M.J. O'Neill, M.F. Piszczor, M.I. Eskenazi, A.J. McDanal, P.J. George, M.M. Botke, H.W. Brandhorst, D.L. Edwards, D.T. Hoppe, Proc. SPIE, **5179**, 116 (2003). DOI: 10.1117/12.505801

[9] *Handbook of concentrator photovoltaic technology*, ed. by C. Algora, I. Rey-Stolle (John Wiley & Sons, 2016). DOI: 10.1002/9781118755655

[10] V.A. Grilikhes, M.Z. Shvarts, A.A. Soluyanov, E.V. Vlasova, V.M. Andreev, in *Proc. of the Fourth Int. Conf. on Solar Concentrators for the Generation of Electricity or Hydrogen* (El Escorial, Spain, 2007), p. 49–52.

[11] M.Z. Shvarts, M.V. Nakhimovich, N.A. Sadchikov, A.A. Soluyanov, AIP Conf. Proc, **2298**, 050005 (2020). lDOI: 10.1063/5.0032804

[12] N.A. Sadchikov, A.V. Andreeva, Tech. Phys. Lett., **49** (12), 53 (2023). DOI: 10.61011/TPL.2023.12.57585.173A.

[13] M. Meusel, B. Fuhrmann, S. van Riesen, A. Berg, W. Köstler, W. Guter, F. Dunzer, T. Torunski, in *12th European Space Power Conf.* (Juan-les-Pins, France, 2019).

[14] W. Guter, F. Dunzer, L. Ebel, K. Hillerich, W. Köstler, T. Kubera, M. Meusel, B. Postels, C. Wächter, E3S Web Conf., **16**, 03005 (2017). DOI: 10.1051/e3sconf/20171603005

Translated by D.Safin